

# CIRCULAR ECONOMY APPROACH FOR TREATMENT OF WATER-CONTAINING DICLOFENAC USING RECYCLABLE MAGNETIC Fe<sub>3</sub>O<sub>4</sub> NANOPARTICLES: A CASE STUDY OF REAL WATER SAMPLE FROM LAKE VICTORIA

## **Abstract**

**Aims:** A circular economy is a concept that aims to create a sustainable future by reducing waste and promoting the reuse of resources. In the field of water treatment, this concept has been applied through the use of recyclable materials to remove pollutants from water.

**Place and Duration of Study:** In this study, we investigated the use of recyclable magnetic Fe<sub>3</sub>O<sub>4</sub> nanoparticles to remove diclofenac from a water sample from Lake Victoria. The water sample was collected once to test the application of recyclable magnetic Fe<sub>3</sub>O<sub>4</sub> nanoparticles in real environmental samples.

**Methodology:** The nanoparticles were synthesized using a coprecipitation method and characterized using various techniques, including SEM/EDX, XRD, MPMS, ImageJ, and Solid addition method for PZC determination. The removal of diclofenac experiments was designed by response surface methodology.

**Results:** The optimal conditions for diclofenac removal were pH 2, concentration 500 ug/L, contact time 60 minutes, and adsorbent dose 50 mg with a removal percentage of 69.95%. The reusability of the Fe<sub>3</sub>O<sub>4</sub> nanoparticles was evaluated for three cycles, with removal percentages of 69.95%, 60%, and 41.6% for the first, second, and third cycles, respectively. This characteristic aligns with the principles of the circular economy, promoting resource conservation and waste reduction. The nanoparticles were also tested on a real water sample from Lake Victoria, resulting in 100% removal of diclofenac.

**Conclusion:** This finding suggests that the Fe<sub>3</sub>O<sub>4</sub> nanoparticles can be adopted for drinking water treatment in the East African community, addressing the issue of pharmaceutical contamination in water bodies.

**Keywords:** Waste reduction, material recycling, magnetic Fe<sub>3</sub>O<sub>4</sub> nanoparticles, Circular economy, Lake Victoria Water

## **1.0 INTRODUCTION**

Lake Victoria, located in East Africa, serves as a crucial freshwater resource for approximately 40 million people in Uganda, Kenya, and Tanzania [1]–[5]. It is a vital water resource for millions of people in East Africa, providing drinking water, supporting agriculture, and sustaining aquatic life [1], [3], [5]. However, recent studies have reported the presence of diclofenac in water samples collected from various locations within Lake Victoria, indicating the contamination of this important water body [5], [6]. The presence of diclofenac in Lake Victoria poses potential risks to both human and ecological health, emphasizing the urgent need for effective removal strategies [7] [5], [6]. Conventional treatment methods, such as activated carbon adsorption, advanced oxidation processes, and membrane filtration, have shown limitations in terms of efficiency, cost-effectiveness, and the generation of secondary waste [8]. In light of these challenges, utilising magnetic nanoparticles offers a promising alternative for removing diclofenac from water [9], while aligning with the principles of circular economy.

In recent years, the circular economy has emerged as a promising approach to address environmental challenges and promote economic growth and resource efficiency [10]. The circular economy provides a fresh approach to sustainable development by highlighting the significance of reusing, recycling, and recovering materials [11]. Recently, researchers have advocated for the incorporation circular economy in water and wastewater sector with more emphases on water reuse, nutrients recovery, energy recovery, metals and precious metals recovery and other valuable materials[12]–[16]. In line with the above emphases, some water sectors in countries like Finland [17], Sweeden [17], and Australian [18] have been practicing circular economy. However, there was no emphases by the above researchers on the need for a rethink on the development of new technology and materials that are recyclable in nature to be applied in water and wastewater treatment. Magnetic nanoparticles are recyclable materials that need to be adopted in circular economy of water. These materials are capable of removing various contaminants, including heavy metals, organic pollutants, and bacteria, from water and wastewater through several mechanisms such as adsorption, coagulation, and photocatalysis [9], [19]. Magnetic nanomaterials have an advantage over other materials because they can be easily separated from treated water by applying an external magnetic field [19]. This makes the separation process less expensive and complex. Additionally, magnetic nanoparticles can be reused multiple times, which reduces waste generation. In contrast, other materials used in traditional water treatment, which follow the linear economy principle, lead to higher sludge production. Furthermore, magnetic nanomaterials can help reduce the amount of chemicals needed for water and wastewater treatment [19]. For instance, using magnetic iron oxide nanoparticles as a coagulant can decrease the amount of iron salts required for coagulation, resulting in less sludge generated during treatment.

Magnetic nanoparticles, particularly magnetic iron oxide ( $\text{Fe}_3\text{O}_4$ ) nanoparticles, have gained attention for their exceptional properties such as high surface area, magnetic responsiveness, and stability, making them ideal for pollutant removal [9]. Furthermore, their recyclability aligns with circular economy principles that prioritize continuous material reuse or recovery instead of waste disposal. The schematic representation of  $\text{Fe}_3\text{O}_4$  nanoparticles for treatment of diclofenac which aligns with circular economy principles is shown in Figure 1. Thus, the aim of this study is to investigate the efficacy and reusability of  $\text{Fe}_3\text{O}_4$  nanoparticles in removing diclofenac from polluted water, with a focus on the potential benefits of adopting circular economy principles in water treatment practices. The process optimization was done by response surface methodology.

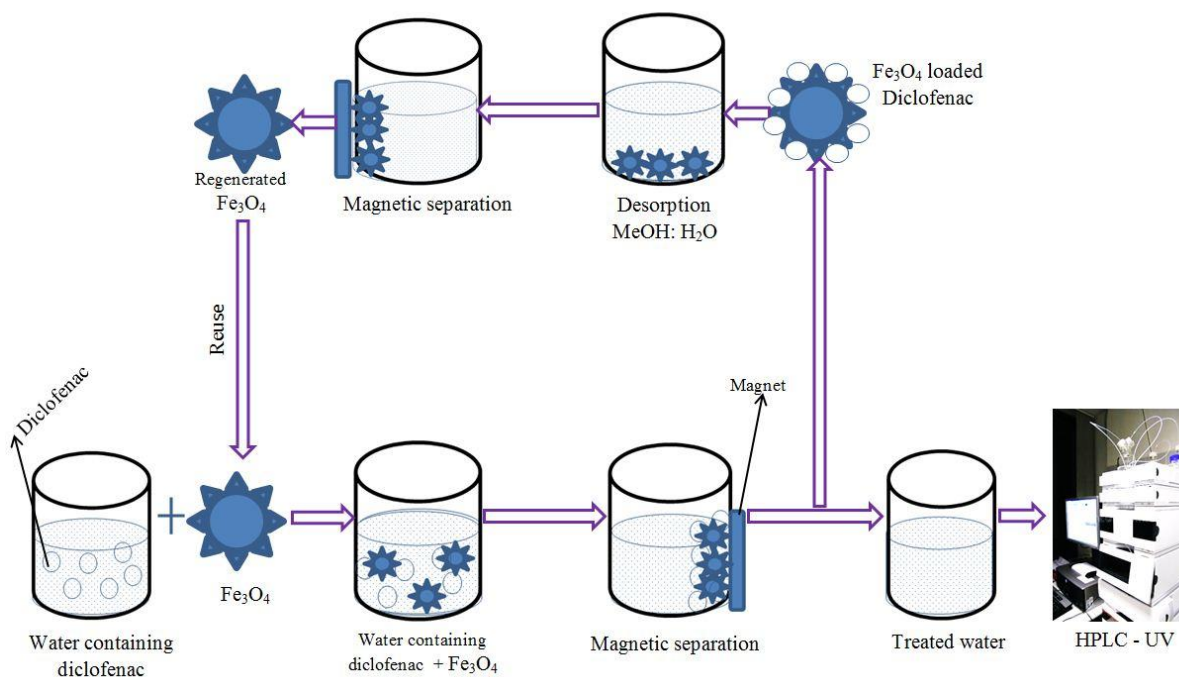


Fig.1. Circular economy application in water treatment Using recyclable magnetic  $\text{Fe}_3\text{O}_4$  nanoparticles

## 2.0 METHODOLOGY

## 2.1 Chemicals/Reagents

Various chemicals and reagents to be used in this research are deionized water, ethanol, Diclofenac (DCF), Ammonium solution ( $\text{NH}_4\text{OH}$ ),  $\text{FeCl}_2$ , iron (III) chloride hexahydrate ( $\text{FeCl}_3 \cdot 6\text{H}_2\text{O}$ ),  $\text{H}_2\text{SO}_4$ , ortho phosphoric acid, ethylenediaminetetraacetate sodium salt ( $\text{Na}_2\text{EDTA}$ ), and glass fiber filter. Milli Q water (HPLC grade) was obtained from Carlo Erba reagents S.A.S. (France). Methanol and acetonitrile (HPLC grade) were purchased from Carl Roth GmbH and Co. KG (Germany).

## 2.2 Study area and sampling

A water sample was obtained from Gaba, Murchison Bay, Lake Victoria, Uganda, as shown in Figure 2. Five samples were collected from different points and combined into a 2L amber bottle. The site was chosen due to high human settlement and commercial activities. The sample was kept in ice and transported to the laboratory within 30 minutes. Water quality measurement and extraction were performed immediately upon arrival at the laboratory.

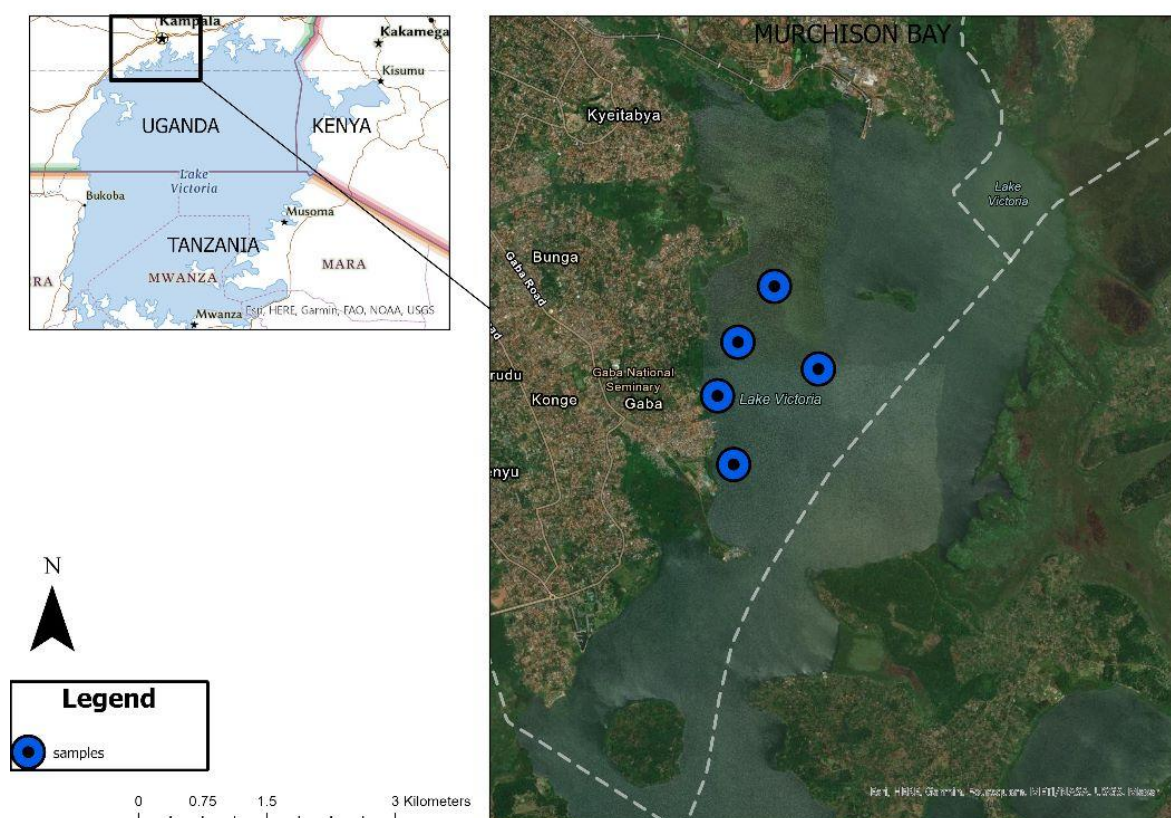


Fig. 2. Map of Lake Victoria indicating Gaba, Uganda

## 2.3 Synthesis of $\text{Fe}_3\text{O}_4$ nanoparticles

The  $\text{Fe}_3\text{O}_4$  nanoparticles were synthesized by coprecipitation of iron (II) and iron (III) salt using ammonium solution [20]. In brief, Iron (II) chloride (3.31 g,  $\text{FeCl}_2$ ) and iron (III) chloride (6.17 g,  $\text{FeCl}_3 \cdot 6\text{H}_2\text{O}$ ) was diluted in 200 ml of deionized water at a molar ratio of 1:2. Then, the content was stirred at 200 revolutions per minute (rpm) using mechanical stirrer for 150 minutes with the simultaneous addition of ammonium hydroxide solution to a pH 10. The entire synthesis procedure was carried out under nitrogen gas to prevent oxidation. The black precipitate was formed which indicates the formation of  $\text{Fe}_3\text{O}_4$  nanoparticles. The nanoparticles were separated by applying an external magnetic field. Then, the nanoparticles were washed with distilled water and ethanol. Finally, the nanoparticles were dried at  $70^\circ\text{C}$  in a hot air oven for 5 hours.

## 2.4 Characterizations

The surface morphology of the  $\text{Fe}_3\text{O}_4$  nanoparticles was examined using scanning electron microscopy coupled with energy dispersed x-ray (Sigma 300 VP, ZEISS) and X-ray diffraction (XRD)

patterns were analyzed using a Rigaku Miniflex 600. Ultraviolet-visible adsorption spectral measurements were conducted using a UV-Vis absorption spectrometer (Jenway 7315) to evaluate the energy band gap using Tau's equation. A magnetic curve was generated using a magnetic properties measuring system (MPMS, MultiVu, Version 1.5) at 5 K temperature. The point of zero charge (pHpzc) of the magnetic Fe<sub>3</sub>O<sub>4</sub> nanoparticles was determined using 0.01 M NaCl aqueous solutions at pH 1, 5, 7, 8, 10, and 12. These pH values were adjusted using either a 0.1N HCl or a 0.1N NaOH aqueous solution. The pHpzc value was calculated from a plot of pHf-pHi vs pHi, where pHf is the final pH and pHi is the initial pH. The pHpzc can be obtained at the point where the line of the final pHf-pHi crosses the line of the starting pHi [21].

## 2.5 Response surface methodology and adsorption experiments

The experiments were carried out using Design Expert 13.0 software and followed the central composite design (CCD) of the response surface methodology (RSM). The study aimed to investigate the removal of diclofenac from aqueous solution using four operating variables: contact time (10-60 minutes), concentration (500-2100 ug/L), adsorbent dose (10-50 mg), and pH (2-11). Adsorption experiments were conducted in a 50-mL glass conical flask with 20 mL of diclofenac solution at a known concentration, pH, time, and adsorbent dose. The pH was adjusted using 0.1M NaOH and 0.1M HCL. All runs were conducted at room temperature (25°C) using a magnetic stirrer with a shaking speed of 150 rpm for all conditions.

## 2.6 Extraction of Water sample

Solid phase extraction was utilized to obtain diclofenac from a water sample. The process began by filtering 2L of the water sample through a 1.0 um glass fiber filter. Afterwards, 100 um of a solution containing 40% sulphuric acid and 0.6 g of ethylenediaminetetraacetate sodium salt (Na<sub>2</sub>EDTA) were added to the filtrate, and the bottle was stirred for 30 minutes to ensure complete dissolution of Na<sub>2</sub>EDTA. Then, 50 umL of 1000 ug/L trifloxystrobin was added as an internal standard for calibration and to account for possible matrix effects. The cartridges were pre-conditioned with 5 mL of methanol and 5 mL of deionized water at a flow rate of 1 mL per minute. Water samples were passed through the cartridges at 10 mL per minute. The cartridges were rinsed with 5 mL of milli Q water to remove excess Na<sub>2</sub>EDTA, and elution was performed with 2 x 4 mL of methanol at 1 mL per minute. Finally, the extract was evaporated using a nitrogen stream and reconstituted with 1 mL of methanol-water (25:75, v/v).

## 2.7 Analytical method

The concentration of diclofenac was analyzed by an HPLC (Shimadzu 223-60140A) equipped with an RP-18e (100 x 4.6 mm) and UV detector at 275 nm. The column was at 30 oC during the sample analysis. The mobile phase consists of 0.1 % of ortho phosphoric acid (A) and acetonitrile (B) at constant flow rate of 1.5mL per minutes. The total run time for each sample is 8 minutes and retention time was found to be 4.776 minutes.

## 2.8 Adsorption kinetics and isotherms experiments

The optimization study involved analyzing the data from batch runs to identify the best combination of variables for optimal removal of diclofenac from water. The optimal conditions were then used for kinetic and equilibrium studies. Kinetic studies were conducted by varying the contact time under optimal conditions, and the resulting data were used to determine the equilibrium time. The data were then fitted to different kinetic models, such as the pseudo-first order, and pseudo-second order. The adsorption isotherm was determined by agitating diclofenac solutions with different initial concentrations at the equilibrium time, using the optimal pH and adsorbent dose. The initial concentrations and corresponding adsorption capacities were then fitted to Langmuir and Freundlich isotherm models.

## 2.9 Reusability of Fe<sub>3</sub>O<sub>4</sub> nanoparticles for diclofenac removal

To conduct reusability studies for diclofenac removal, roughly 200 mg of Fe<sub>3</sub>O<sub>4</sub> nanoparticles were placed into a 100 mL beaker, and 5 mL of methanol:water (50:50, v/v) was added. The mixture was agitated at 100 rpm for 20 minutes using an orbital shaker. The nanoparticles were then separated from the mixture using an external magnetic field and dried in an oven at 70°C for 2 hours. The experimental setup was carried out using optimal conditions for diclofenac removal, which included a pH of 2, a concentration of 500 ug/L, an adsorbent dose of 50 mg, and agitation at 180 rpm for 60

minutes using an orbital shaker. After this, the nanoparticles were again separated from the solution using an external magnetic field and the remaining diclofenac concentration was analyzed by HPLC (Shimadzu, 223-60140A). This process was repeated for three cycles.

### 3.0 RESULTS AND DISCUSSION

#### 3.1 Characterizations results

The characterization results of the  $\text{Fe}_3\text{O}_4$  nanoparticles are presented in Figure 3 (a-f). The morphology indicate that  $\text{Fe}_3\text{O}_4$  nanoparticles have irregular shape, Figure 5a and the elemental composition showed that it contains Fe and  $\text{O}_2$  atom with weight percentage of 54.94 and 45.1 respectively, Figure 3b. The particles size distribution was determined using imageJ with aid of images obtained from SEM and the average particles size was found to be 25.16 nm, Figure 3c. The magnetic properties of  $\text{Fe}_3\text{O}_4$  nanoparticles were investigated by MPMS at 5K temperature (Figure 5d). As can be seen in Figure 3d, the value of saturation magnetization ( $M_s$ ) of  $\text{Fe}_3\text{O}_4$  nanoparticles was equal to 70 emu/g, with s-curve shape indicating the supermagnetic properties of the nanoparticles. This amount of  $M_s$  allows the nanoparticles to be easily separated from the water by a magnet after the adsorption process is complete [20]. Also, collecting the magnetic nanoparticles from water does not require time-consuming and costly methods such as filtration and centrifugation and will not cause secondary pollution in the environment and can be reused for later stages and recycled.

The PZC (Point of Zero Charge) of  $\text{Fe}_3\text{O}_4$  nanoparticles refers to the pH at which the surface charge of the nanoparticles is neutral. The PZC of  $\text{Fe}_3\text{O}_4$  nanoparticles was found to be 6.94, Figure 3e. Below and above the PZC, the surface of  $\text{Fe}_3\text{O}_4$  nanoparticles carries a net positive and negative charge, respectively [21]. The XRD pattern of  $\text{Fe}_3\text{O}_4$  of nanoparticles is presented in Figure 3f. The diffraction peaks at 2theta position of  $20.1^\circ$ ,  $30.464^\circ$ ,  $35.893^\circ$ ,  $43.485^\circ$ ,  $53.905^\circ$ ,  $57.476^\circ$ , and  $63.064^\circ$  correspond to miller indices of 111, 220, 311, 400, 422, 511, and 440 respectively. Also, the crystal structure of  $\text{Fe}_3\text{O}_4$  nanoparticles was found to be cubic with space group of 227: Fd-3m:1. Thus, the XRD indicate the formation of single crystal phase. Similarly, the crystallographic information of  $\text{Fe}_3\text{O}_4$  nanoparticles with JCPDS NO. 65-3107 has been reported by [22].

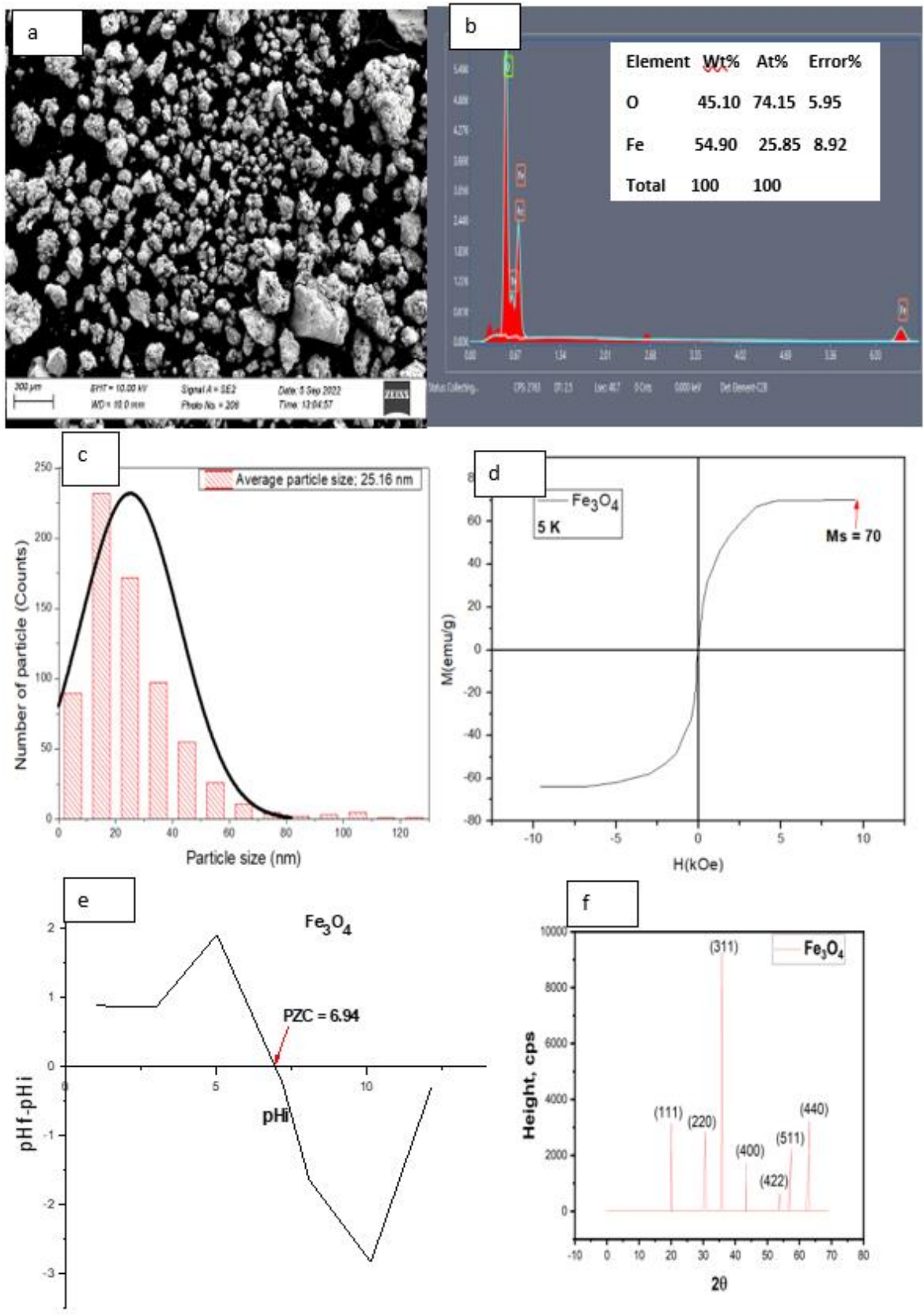


Fig. 3. Characterization results

### 3.2 Modeling and optimization studies

Table 1 presents the percentage of diclofenac removal using CCD. The diclofenac removal efficiency ranges from 7.12 to 75.962 %. The equation for quadratic model is given equation 1. The quadratic model's suitability was validated through ANOVA analysis, as shown in Table 2. The F-value of 265.33 indicates that the model is significant (p-value 0.0001), and the p-values less than 0.05 indicate which model terms are significant, including A, B, C, D, BC, BD, CD, A2, B2, and D2. The lack-of-fit F-value of 4.45 implies that the lack of fit is not significant (p-value = 0.0567) relative to pure error, confirming the quadratic model's applicability. Fit statistics in Table 3 validate the model, with a predicted R<sup>2</sup> of 0.9754 in reasonable agreement with the adjusted R<sup>2</sup> of 0.9922 (i.e., the difference is less than 0.2). The Adeq Precision measures the signal to noise ratio, with a ratio greater than 4 being desirable. The ratio of 61.330 indicates an adequate signal, and diagnostic statistics such as predicted vs actual plot, normal probability plot, predicted vs runs and predicted vs actual confirmed the adequacy of the model (Figure 4).

Figure 5 shows the 3D response surface plots that illustrate how the experimental parameters, namely concentration, contact time, adsorbent dose, and pH, interact to affect diclofenac removal. High removal percentages are achieved when the pH and concentration are minimized while the adsorbent dose and contact time are increased. The optimal value for each parameter was determined numerically using Design Expert 13.0 by setting the appropriate goal or criteria. Based on the analysis using CCD and RSM, the predicted response value for diclofenac removal percentage using optimal conditions (pH = 2, concentration = 500 mg/L, contact time = 60 minutes, and adsorbent dose = 50 mg) was 71.55%, with a desirability of 1.0 (Figure 6). Verification experiments resulted in 69.95% diclofenac removal at the same optimal conditions, indicating good agreement with the generated quadratic model and confirming its robustness.

$$\% \text{Removal of diclofenac} = 31.2 - 1.81422 * A - 9.98917 * B + 3.07528 * C - 19.9247 * D - 0.235312 * AB - 0.344813 * AC + 0.659813 * AD - 1.96944 * BC - 3.35856 * BD - 1.64531 * CD + 3.18067 * A^2 - 2.23283 * B^2 + 4.12617 * C^2 + 4.61517 * D^2 \quad (1)$$

Table 1. Experimental runs and its percentages

Run	Factor 1	Factor 2	Factor 3	Factor 4	Response	
	A:Time Minutes	B:Concentration ug/L	C:Adsorbent dose mg	D:pH	Actual removal %	Predicted %
1	60	2000	10	2	48.521	49.07
2	35	1250	30	6.5	32.24	31.20
3	60	2000	50	11	7.12	5.34
4	60	2000	10	11	7.623	7.11
5	35	1250	50	6.5	38.719	38.40
6	60	1250	30	6.5	31.353	32.57
7	35	1250	30	6.5	31.44	31.20
8	10	2000	10	11	7.914	9.20
9	10	500	10	2	61.349	62.65
10	60	500	50	11	35	36.45
11	10	2000	50	2	60	59.99
12	35	1250	30	11	14.021	15.89
13	10	2000	50	11	8	8.81
14	35	500	30	6.5	37	38.96
15	60	500	50	2	73.316	71.55
16	60	500	10	2	59.428	58.86
17	10	500	50	11	40	38.98

18	35	1250	10	6.5	30.999	32.25
19	35	1250	30	6.5	30.88	31.20
20	60	2000	50	2	52	53.88
21	10	1250	30	6.5	36.474	36.19
22	10	500	10	11	33.123	31.49
23	10	500	50	2	75.962	76.72
24	35	1250	30	6.5	30.568	31.20
25	35	1250	30	6.5	31.84	31.20
26	35	2000	30	6.5	20	18.98
27	35	1250	30	2	56.675	55.74
28	10	2000	10	2	55	53.80
29	35	1250	30	6.5	33.035	31.20
30	60	500	10	11	30.805	30.34

Table 2. ANOVA for Quadratic model

Source	Sum of Squares	df	Mean Square	F-value	p-value	
<b>Model</b>	10062.12	14	718.72	265.33	< 0.0001	significant
A-Time	59.25	1	59.25	21.87	<b>0.0003</b>	
B-Concentration	1796.10	1	1796.10	663.06	< <b>0.0001</b>	
C-Adsorbent dose	170.23	1	170.23	62.84	< <b>0.0001</b>	
D-pH	7145.90	1	7145.90	2638.01	< <b>0.0001</b>	
AB	0.8860	1	0.8860	0.3271	0.5759	
AC	1.90	1	1.90	0.7023	0.4152	
AD	6.97	1	6.97	2.57	0.1297	
BC	62.06	1	62.06	22.91	<b>0.0002</b>	
BD	180.48	1	180.48	66.63	< <b>0.0001</b>	
CD	43.31	1	43.31	15.99	<b>0.0012</b>	
A <sup>2</sup>	26.21	1	26.21	9.68	0.0072	
B <sup>2</sup>	12.92	1	12.92	4.77	0.0453	
C <sup>2</sup>	44.11	1	44.11	16.28	0.0011	
D <sup>2</sup>	55.19	1	55.19	20.37	0.0004	
<b>Residual</b>	40.63	15	2.71			
Lack of Fit	36.52	10	3.65	4.45	0.0567	not significant
Pure Error	4.11	5	0.8217			
<b>Cor Total</b>	10102.75	29				

Table 3. Fit statistics

<b>Std. Dev.</b>	1.65	<b>R<sup>2</sup></b>	0.9960
<b>Mean</b>	37.01	<b>Adjusted R<sup>2</sup></b>	0.9922
<b>C.V. %</b>	4.45	<b>Predicted R<sup>2</sup></b>	0.9754

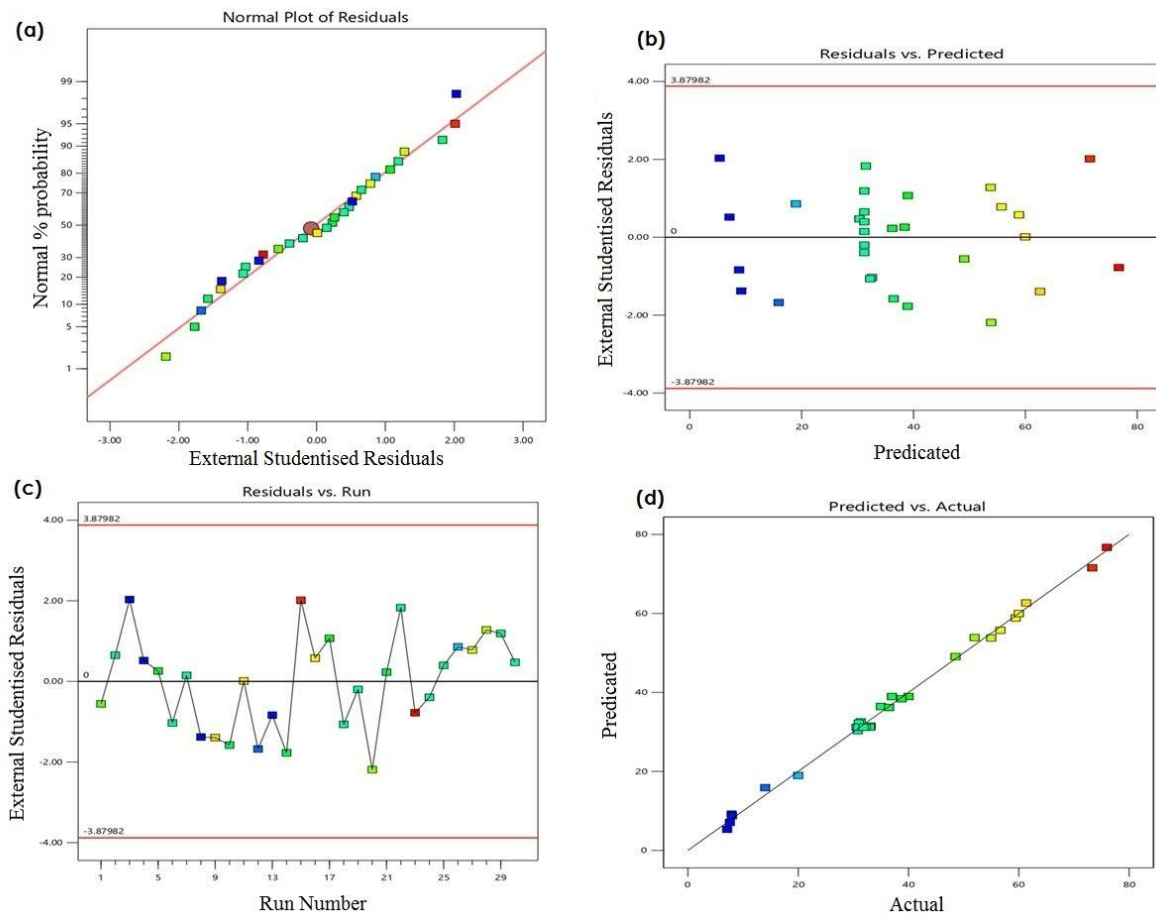


Fig. 4. Diagnostic statistics, (a); Normal plot residuals, (b); Residuals vs predicted, (c); Residuals vs run and (d); Predicted vs actual

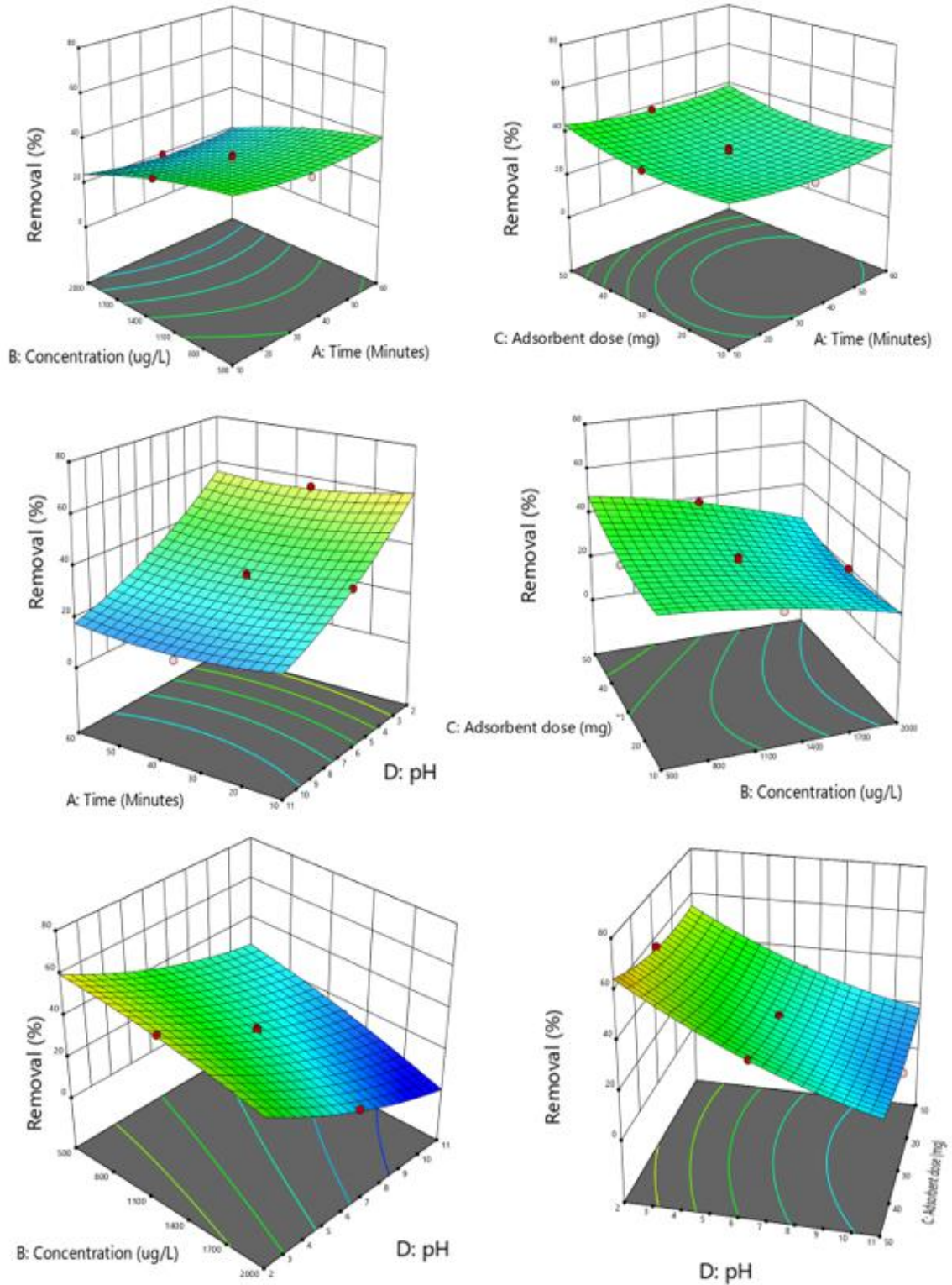


Fig. 5. Three-dimensional surface plots showing interactions of variables: (a) concentration, time; (b) adsorbent dose, time; (c) time, pH; (d) adsorbent, concentration; (e) concentration, pH; (f) pH, adsorbent

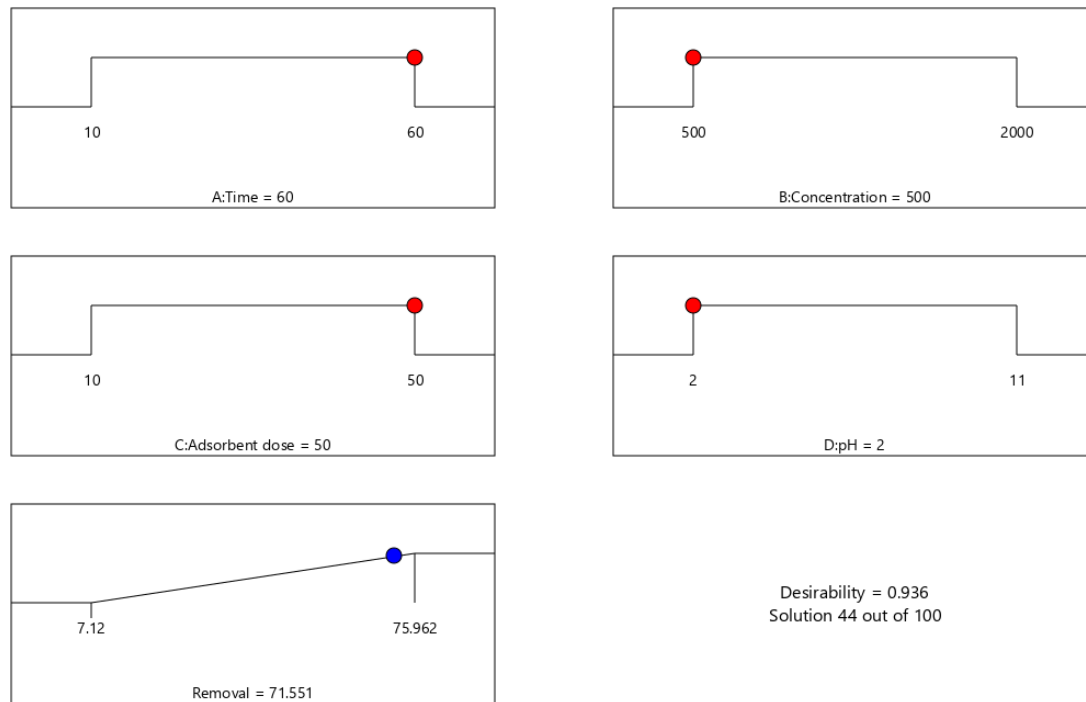


Fig. 6. Optimization

### 3.3 Reusability of Fe<sub>3</sub>O<sub>4</sub> nanoparticles for diclofenac removal

The reusability of Fe<sub>3</sub>O<sub>4</sub> nanoparticles for diclofenac removal is a promising approach towards a circular economy. The ability to reuse the nanoparticles for multiple cycles is a significant step towards reducing waste and increasing resource efficiency.

The first cycle resulted in a diclofenac removal rate of 69.5%, demonstrating that the nanoparticles effectively removed the contaminant, Figure 7. However, the removal efficiency decreased to 60% and 41.6% in the second and third cycles, respectively. While the removal efficiency decreased with each cycle, it is still noteworthy that the nanoparticles could be used for multiple cycles, which reduces the need for new materials and resources. Moreover, the decrease in removal efficiency with each cycle indicates that the nanoparticles' surface properties may have changed over time. This could be due to the accumulation of diclofenac on the surface or other contaminants in the water. To improve the reusability of these nanoparticles, further research is needed to investigate ways to maintain their surface properties and increase their durability.

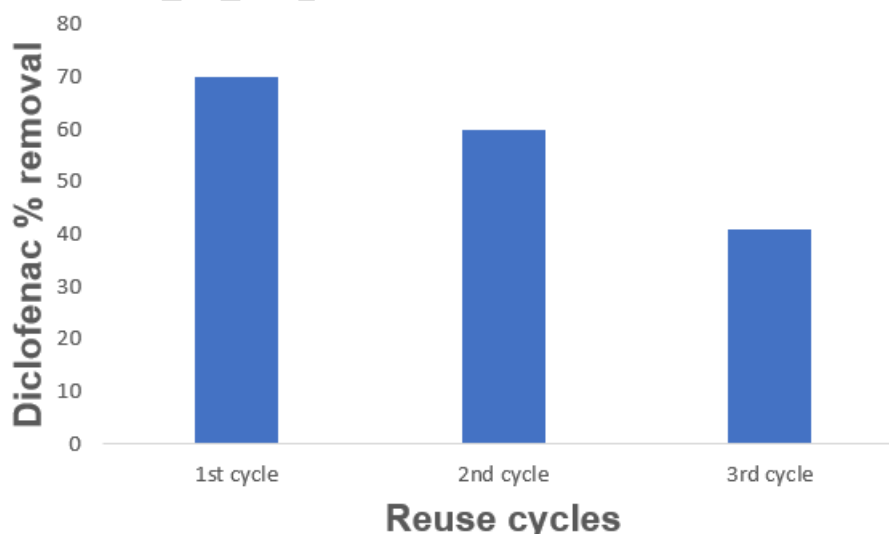


Fig. 7. Reusability studies

### 3.4 Removal of diclofenac from real water sample from Lake Victoria

The removal of diclofenac from Lake Victoria water samples is a crucial step towards ensuring the safety of drinking water for millions of people in Uganda, Kenya, and Tanzania. The presence of diclofenac in water bodies can have negative impacts on aquatic life and can also affect human health. The diclofenac concentration in the Lake victoria was analyzed and presented in Table 4. The diclofenac concentration was 1.6363 ug/L, which is relatively low but still a cause for concern. When the optimal conditions of pH 2, concentration 500 ug/L, adsorbent dose, and time 60 minutes were applied to 20 mL of the Lake water sample, the removal efficiency of diclofenac was 100%. This indicates that Fe<sub>3</sub>O<sub>4</sub> nanoparticles can effectively remove diclofenac from Lake Victoria water sample, Table 4. The removal of diclofenac from wastewater samples as reported by Soares et al. were found between 20 to 41 % and this indicate that the current is favourable due to its 100 % removal efficiency[9].

This is significant for the circular economy as it ensures that water remains safe and free from contaminants (such as diclofenac). Also, the circular economy is an economic system that aims to keep products, components, and materials at their highest utility and value at all times. The removal of diclofenac from Lake Victoria water samples contributes to this by ensuring that the water remains a valuable resource that can be used for various purposes, including drinking, irrigation, and other domestic uses.

Table 4. Removal of diclofenac from Lake water sample

Conc. diclofenac Lake Water	of in	Time (Minutes)	Adsorbent (mg)	pH	Removal (%)
1.6363		60	50	2	100

### 3.5 Kinetic studies

In the adsorption process, kinetic studies provide information about optimum conditions, mechanism of sorption, and possible rate-controlling step [23]. The most commonly used kinetics models are Pseudo-first order and Pseudo-second order kinetic models, which are represented in equation 2 and 3, respectively.

$$\text{Log}(q_e - q_t) = \text{Log } q_e - \frac{K_1 t}{2.303} \quad (2)$$

Where

$K_1$  (1/min) is the pseudo first order adsorption rate coefficient,  $q_e$  and  $q_t$  are the values of amount adsorbed per unit mass at equilibrium and at any time  $t$ ,

For pseudo first order, the plot of  $\text{Log}(q_e - q_t)$  against time ( $t$ ) gives a linear graph from which  $K_1$  and  $q_e$  can be determined from the slope and intercept of the plot, respectively.

$$\frac{t}{q_t} = \frac{1}{K_2 q_e^2} - \frac{1}{q_e} t \quad (3)$$

Where,

$q_e$  and  $q_t$  are the values of amount adsorbed per unit mass at equilibrium and at any time  $t$ ,  
 $K_2$  (g/mg min.) is the rate constant of second-order adsorption

For pseudo second order, the plot of  $\frac{t}{q_t}$  against time (t) gives a linear graph from which  $q_e$  and  $K_2$  can be determined from the slope and intercept of the plot, respectively.

The pseudo-second order kinetic model for diclofenac removal was analyzed, and the results are presented in Figure 8a. The  $R^2$  value for the linear plot of this model is 1, indicating a strong correlation. The calculated adsorption capacity at equilibrium ( $q_e = 37.739$  mg/g) closely matches the experimental value ( $q_{e,calc} = 37.36$  mg/g) for the pseudo-second order model. The rate constant of pseudo-second order kinetic was found to be 1.756 mg/g.minutes. On the other hand, Figure 8b shows a linear plot of the pseudo-first order kinetic fit for diclofenac removal using  $Fe_3O_4$  nanoparticles. However, the coefficient of determination ( $R^2 = 0.7984$ ) for this model is relatively low, suggesting that the diclofenac removal process with  $Fe_3O_4$  nanoparticles does not follow the pseudo-first order kinetic model. The rate constant of pseudo-first order kinetic was found to be 0.00622 per minutes. The results indicate that the pseudo-second order model provides a better correlation for the adsorption of diclofenac onto  $Fe_3O_4$  nanoparticles compared to the pseudo-first order model. This adsorption process follows pseudo-second order kinetics and involves chemisorption. **Similar studies using different magnetic adsorbents have also shown good fitting with pseudo-second order kinetics[24].**

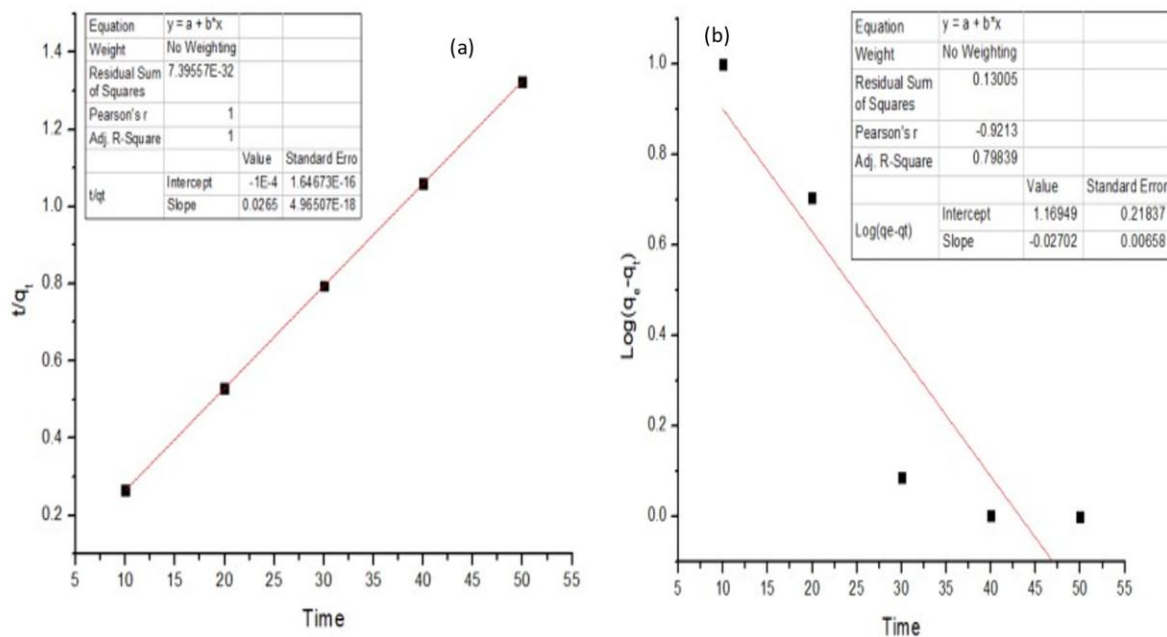


Figure 8; Kinetics; (a) Pseudo second order (b) Pseudo first order

### 3.6 Isotherm studies

Langmuir and Freundlich isotherms were used to investigate the relationship between the magnetic  $Fe_3O_4$  nanoparticles and the diclofenac. Langmuir isotherm model assumes monolayer adsorption onto a surface containing a finite number of adsorption sites of uniform strategies of adsorption with no transmigration of adsorbate in the plane of surface [25]. It is expressed by the equation 4;

$$\frac{C_e}{q_e} = \frac{1}{K_L q_{max}} + \frac{1}{q_{max}} \cdot C_e \quad (4)$$

Where

$C_e$  = the equilibrium concentration of adsorbate (mg/L).

$q_e$  = the equilibrium value of adsorbate adsorbed per unit weight of adsorbent (mg/g).

$q_{max}$  = the maximum amount of adsorption corresponding to monomolecular layer coverage (mg/g).

$K_L$  = the Langmuir constant (l/mg).

A linearized plot of  $\frac{C_e}{q_e}$  against  $C_e$  yields a straight line graph which gives intercept and slope that corresponds to  $\frac{1}{K_L q_{max}}$  and  $\frac{1}{q_{max}}$  respectively, from which the  $q_{max}$  and  $K_L$  can be calculated.

To confirm the favourability of an adsorption process to Langmuir isotherm, the essential features of the isotherm can be expressed in terms of a dimensionless constant known as the separation factor or equation parameter  $R_L$ , which can be calculated by the following equation;

$$R_L = \frac{1}{C_0 K_L}$$

Where,  $C_0$  is the initial concentration

The value of  $R_L$  indicates whether the isotherm is irreversible ( $R_L=0$ ), favourable ( $0 < R_L < 1$ ), linear ( $R_L=1$ ), or unfavourable ( $R_L > 1$ ).

Freundlich isotherm is suitable for adsorption processes that occur on heterogenous surfaces. Freundlich isotherm gives an expression that defines the surface heterogeneity and the exponential distribution of active sites and their energies [26]. It is expressed by the equation 5 below;

$$\text{Log}q_e = \text{Log}K_F + \frac{1}{n}\text{Log}C_e \quad (5)$$

Where,

$q_e$  and  $C_e$  are the equilibrium adsorption capacity of the adsorbent and the equilibrium concentration in the aqueous solution, respectively.

$K$  and  $n$  are the Freundlich constants related to adsorption capacity.

The plot of  $\text{Log}q_e$  against  $\text{Log}C_e$  gives a straight line graph. And the parameters;  $n$  and  $K_L$  was calculated from the slopes and intercept of the graph.

In Figure 9a, the Langmuir model displays a linear plot of  $C_e/q_e$  against  $C_e$ , with an  $R^2$  value of 0.9973, indicating that the adsorption process fits the model. The maximum adsorption value,  $q_{\text{max}}$ , is 91.158 mg/g. The values of  $K_L$  and  $R_L$  are 2.7009 and 0.523, respectively. The  $R_L$  value of 0.523 indicate that the adsorption process is favourable. On the other hand, Figure 9b shows the Freundlich model's plot of  $\text{log}q_e$  against  $\text{log}C_e$ , with an  $R^2$  value of 0.9327, which is lower than that of the Langmuir model (0.98068). According to the  $R^2$  value, the Freundlich model is unsuitable for describing the experimental data for diclofenac adsorption onto  $\text{Fe}_3\text{O}_4$  nanoparticles. The values of  $K_F$  and  $n$  are calculated from the intercept and slope of the linearized Freundlich model are 3.819 and 2.444. Similarly, Soares et al reported that removal of diclofenac magnetic nanoparticles follows Langmuir isotherm[9].

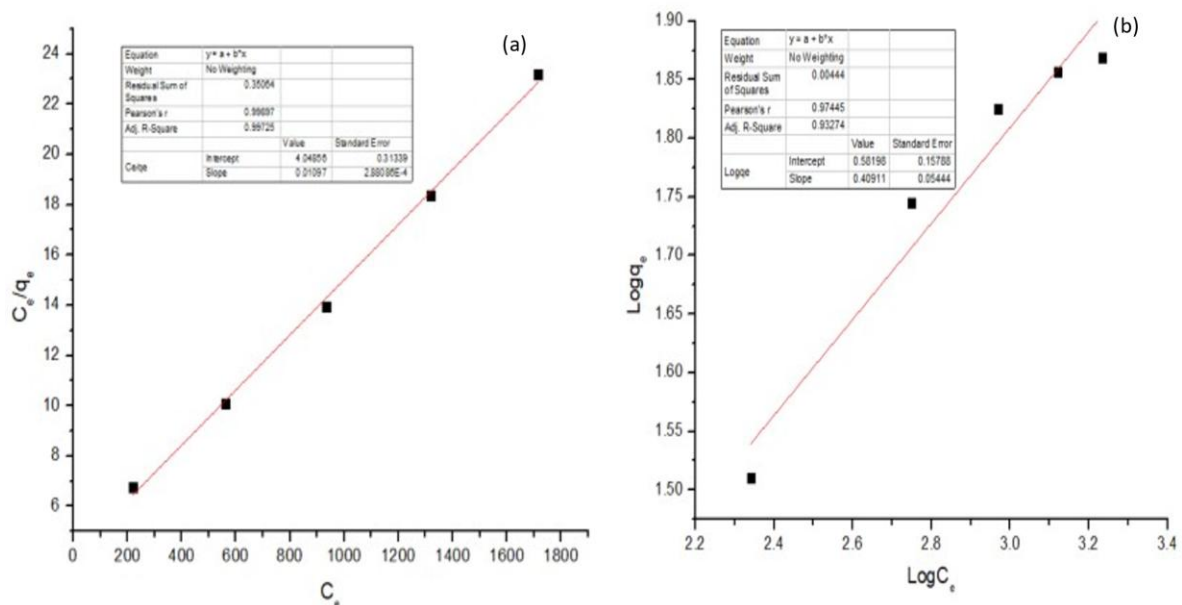


Figure 9; Isotherms graphs: (a) Langmuir isotherm (b) Freundlich isotherm

### 3.7 Mechanism of adsorption

To understand the mechanism of adsorption, the nature of  $\text{Fe}_3\text{O}_4$  nanoparticles and diclofenac at various pH must be known. From Figure 3e, the point of zero charge (PZC) of  $\text{Fe}_3\text{O}_4$  nanoparticles is

6.94. At pH below 6.94, the surface of  $\text{Fe}_3\text{O}_4$  is positively charged due to the protonation of surface hydroxyl groups. Whereas, at the pH above 6.94, the surface of  $\text{Fe}_3\text{O}_4$  is positively charged due to the deprotonation of surface hydroxyl groups. The diclofenac's pka is 4.18 and that means that it is neutral molecules at the pH below 4.18. Also, at the pH above 4.18, diclofenac exists as negatively charged molecules.

From the optimal conditions of the study, the highest removal was found at pH 2. Based on the information you provided, the possible mechanism of adsorption of diclofenac on  $\text{Fe}_3\text{O}_4$  at pH 2 can be explained as follows: At pH 2, the surface of  $\text{Fe}_3\text{O}_4$  is positively charged due to the protonation of surface hydroxyl groups. On the other hand, diclofenac is in the form of a neutral molecule, which means it can interact with the positively charged surface of  $\text{Fe}_3\text{O}_4$  through weak van der Waals forces and hydrogen bonding. The weak van der Waals forces arise due to the interaction between temporary or permanent dipoles in the  $\text{Fe}_3\text{O}_4$  surface and diclofenac molecule. The Formation of hydrogen bonds is between the oxygen atoms in diclofenac and the surface hydroxyl groups on  $\text{Fe}_3\text{O}_4$ . Unlike this research, the adsorption mechanism of diclofenac and quaternary magnetic nanoparticles was reported to be electrostatic interactions[9].

#### 4.0 CONCLUSION

Circular economy is an approach that aims to reduce waste and promote the efficient use of resources. In the context of water treatment, circular economy principles can be applied to the development of sustainable and cost-effective solutions for removing contaminants from water sources. The use of Recyclable Magnetic  $\text{Fe}_3\text{O}_4$  nanoparticles for the removal of diclofenac from water is an example of such a solution.

The results of the study show that Recyclable Magnetic  $\text{Fe}_3\text{O}_4$  nanoparticles can effectively remove diclofenac from water, with a removal percentage of 69.95% at optimal conditions. The reusability of the nanoparticles was also demonstrated, with removal percentages of 69.95%, 60%, and 41.6% for the first, second, and third cycles, respectively. Furthermore, the nanoparticles were able to remove diclofenac from a real water sample from Lake Victoria with 100% efficiency. The study also found that the pseudo-second order model provided a better correlation for the adsorption of diclofenac onto  $\text{Fe}_3\text{O}_4$  nanoparticles compared to the pseudo-first order model. The Langmuir model was also found to fit the data better than the Freundlich model. The mechanism of adsorption was attributed to weak van der Waals forces and hydrogen bonding.

Based on these results, it can be concluded that Recyclable Magnetic  $\text{Fe}_3\text{O}_4$  nanoparticles are a promising solution for removing diclofenac from water sources. The reusability of the nanoparticles makes them a cost-effective option for water treatment. Moreover, using circular economy principles to develop such solutions can contribute to sustainable and efficient water treatment practices.

#### CONSENT (WHERE EVER APPLICABLE)

Not applicable

#### ETHICAL APPROVAL (WHERE EVER APPLICABLE)

Not applicable

#### REFERENCES

- [1] M. Olokotum *et al.*, "A review of the socioecological causes and consequences of cyanobacterial blooms in Lake Victoria," *Harmful Algae*, vol. 96, no. January, p. 101829, 2020, doi: 10.1016/j.hal.2020.101829.
- [2] F. Ligate *et al.*, "Geogenic contaminants and groundwater quality around Lake Victoria goldfields in northwestern Tanzania," *Chemosphere*, vol. 307, no. P2, p. 135732, 2022, doi: 10.1016/j.chemosphere.2022.135732.
- [3] B. M. Simiyu, H. S. Amukhuma, L. Sitoki, W. Okello, and R. Kurmayer,

- “Interannual variability of water quality conditions in the Nyanza Gulf of Lake Victoria, Kenya,” *J. Great Lakes Res.*, vol. 48, no. 1, pp. 97–109, 2022, doi: 10.1016/j.jglr.2021.10.017.
- [4] C. J. Mwita, “Determination of Heavy Metal Content in Water, Sediment and Microalgae from Lake Victoria, East Africa,” *Open Environ. Eng. J.*, vol. 4, no. 1, pp. 156–161, 2011, doi: 10.2174/1874829501104010156.
- [5] F. Nantaba, J. Wasswa, H. Kylin, W. Palm, H. Bouwman, and K. Kümmerer, “Occurrence, distribution, and ecotoxicological risk assessment of selected pharmaceutical compounds in water from Lake Victoria, Uganda,” *Chemosphere*, vol. 239, pp. 1–11, 2020, doi: 10.1016/j.chemosphere.2019.124642.
- [6] S. Dalahmeh, E. Björnberg, A. K. Elenström, C. B. Niwagaba, and A. J. Komakech, “Pharmaceutical pollution of water resources in Nakivubo wetlands and Lake Victoria, Kampala, Uganda,” *Sci. Total Environ.*, vol. 710, pp. 1–8, 2020, doi: 10.1016/j.scitotenv.2019.136347.
- [7] Z. Shehu, G. William, A. Nyakairu, E. Tebandeke, and O. Nelson, “Overview of African water resources contamination by contaminants of emerging concern,” *Sci. Total Environ.*, vol. 852, pp. 1–30, 2022, doi: 10.1016/j.scitotenv.2022.158303.
- [8] L. Rizzo *et al.*, “Consolidated vs new advanced treatment methods for the removal of contaminants of emerging concern from urban wastewater,” *Sci. Total Environ.*, vol. 655, no. August 2018, pp. 986–1008, 2019, doi: 10.1016/j.scitotenv.2018.11.265.
- [9] S. F. Soares, T. Fernandes, M. Sacramento, T. Trindade, and A. L. Daniel-da-Silva, “Magnetic quaternary chitosan hybrid nanoparticles for the efficient uptake of diclofenac from water,” *Carbohydr. Polym.*, vol. 203, pp. 35–44, 2019, doi: 10.1016/j.carbpol.2018.09.030.
- [10] E. Hysa, A. Kruja, N. U. Rehman, and R. Laurenti, “La innovación de la economía circular y el impacto de la sostenibilidad ambiental en el crecimiento económico: un modelo integrado para el desarrollo sostenible,” *Sustain.*, vol. 12, no. 12, 2020.
- [11] C. Afteni, V. Păunoiu, and M. Afteni, “Study on the Transition from the Linear Economy to the Circular Economy,” *Ann. “Dunarea Jos” Univ. Galati, Fascicle V, Technol. Mach. Build.*, vol. 39, no. 1, pp. 49–55, 2022, doi: 10.35219/tmb.2021.1.08.
- [12] P. Morseletto, C. E. Mooren, and S. Munaretto, “Circular Economy of Water: Definition, Strategies and Challenges,” *Circ. Econ. Sustain.*, vol. 2, no. 4, pp. 1463–1477, 2022, doi: 10.1007/s43615-022-00165-x.
- [13] E. Neczaj and A. Grosser, “Circular Economy in Wastewater Treatment Plant—Challenges and Barriers,” *Proceedings*, vol. 2, no. 614, pp. 1–7, 2018, doi: 10.3390/proceedings2110614.
- [14] G. Mannina *et al.*, “Enhancing a transition to a circular economy in the water sector: The eu project wider uptake,” *Water (Switzerland)*, vol. 13, no. 7, pp. 1–18, 2021, doi: 10.3390/w13070946.

- [15] S. Sauv , S. Lamontagne, J. Dupras, and W. Stahel, "Circular economy of water: Tackling quantity, quality and footprint of water," *Environ. Dev.*, vol. 39, pp. 1–10, 2021, doi: 10.1016/j.envdev.2021.100651.
- [16] G. O'Shea, S. Luoto, S. Bor, H. Hakala, and I. B. Nielsen, "The circular water economy and the 'seven C's,'" *Res. Handb. Innov. a Circ. Econ.*, pp. 133–143, 2021, doi: 10.4337/9781800373099.00020.
- [17] S. Lehtoranta *et al.*, "Circular Economy in Wastewater Management—The Potential of Source-Separating Sanitation in Rural and Peri-Urban Areas of Northern Finland and Sweden," *Front. Environ. Sci.*, vol. 10, pp. 1–18, 2022, doi: 10.3389/fenvs.2022.804718.
- [18] C. Oughton, M. Anda, B. Kurup, and G. Ho, "Water Circular Economy at the Kwinana Industrial Area, Western Australia—the Dimensions and Value of Industrial Symbiosis," *Circ. Econ. Sustain.*, vol. 1, no. 3, pp. 995–1018, 2021, doi: 10.1007/s43615-021-00076-3.
- [19] S. K. Fanourakis, J. Pe a-Bahamonde, P. C. Bandara, and D. F. Rodrigues, "Nano-based adsorbent and photocatalyst use for pharmaceutical contaminant removal during indirect potable water reuse," *npj Clean Water*, vol. 3, no. 1, pp. 1–15, 2020, doi: 10.1038/s41545-019-0048-8.
- [20] S. Kandasamy *et al.*, "Hydrothermal liquefaction of microalgae using Fe<sub>3</sub>O<sub>4</sub> nanostructures as efficient catalyst for the production of bio-oil: Optimization of reaction parameters by response surface methodology," *Biomass and Bioenergy*, vol. 131, pp. 1–9, 2019, doi: 10.1016/j.biombioe.2019.105417.
- [21]  . S. Bayazit and  . Kerkez, "Hexavalent chromium adsorption on superparamagnetic multi-wall carbon nanotubes and activated carbon composites," *Chem. Eng. Res. Des.*, vol. 92, no. 11, pp. 2725–2733, 2014, doi: 10.1016/j.cherd.2014.02.007.
- [22] V. Alimohammadi, M. Sedighi, and E. Jabbari, "Optimization of sulfate removal from wastewater using magnetic multi-walled carbon nanotubes by response surface methodology," *Water Sci. Technol.*, vol. 76, no. 10, pp. 2593–2602, 2017, doi: 10.2166/wst.2017.424.
- [23] D. Balarak, F. Bandani, Z. Shehu, and N. J. Ahmed, "Adsorption Properties of Thermally Treated Rice Husk for Removal of Sulfamethazine Antibiotic from Pharmaceutical Wastewater," *J. Pharm. Res. Int.*, no. June, pp. 84–92, 2020, doi: 10.9734/jpri/2020/v32i830475.
- [24] J. M. N. dos Santos, C. R. Pereira, E. L. Foletto, and G. L. Dotto, "Alternative synthesis for ZnFe<sub>2</sub>O<sub>4</sub>/chitosan magnetic particles to remove diclofenac from water by adsorption," *Int. J. Biol. Macromol.*, vol. 131, pp. 301–308, 2019, doi: 10.1016/j.ijbiomac.2019.03.079.
- [25] D. W. Lamayi, Z. Shehu, P. S. Kwarson, and M. Clay, "Aqueous Phase Removal of Fluoride as Fluorosis agent Using Montmorillonite Clay as a Natural Nano-adsorbent," *Nanochemistry Res.*, vol. 3, no. 2, pp. 219–226, 2018, doi: 10.22036/ncr.2018.02.012.
- [26] A. D. N'diaye and M. S. Kankou, "Modeling of adsorption isotherms of pharmaceutical products onto various adsorbents : A Short Review," *J. Mater.*

UNDER PEER REVIEW